

Mineralogical and Geochemical Studies on Some Early Miocene Sediments of Southwestern Sinai, Egypt

Nabil Abd El-Hafez¹, Ahmed Mousa²,
Tarek El-Hariri², Mohamed Abd El-Moghny¹, Hossam Sharaka³

¹Al-Azhar University, Faculty of Science, Geology Department, Cairo, Egypt.

²Egyptian Petroleum Research Institute, Exploration Department, Nasr City, Egypt.

³Egyptian Mineral Resources Authority, Abbassiya, Cairo, Egypt.

Received 8 November 2018, Accepted 12 January 2019

Abstract

The present work provides a comparison and a contrast of the lithostratigraphy, mineralogy, and geochemistry of the early Miocene rocks exposed in El-Markha and Wadi Gharandal sections (Nukhul and Rudeis formations) at Southwest Sinai. Miocene succession of Southwest Sinai is classified from base to top into: Nukhul and Rudeis formations. Rudeis Formation unconformably overlies Nukhul Formation and unconformably underlies Kareem Formation. The Early Miocene sequence revealed the presence of calcite as the dominant minerals in the nonclastic rocks. Quartz is the main mineral in the clastic rocks, while goethite is most important minerals in the iron-rich sand, whereas halite is foremost minerals in evaporate samples. Hematite, kaolinite, halite and gypsum are the secondary minerals constituting the studied rock units with varying amount. The foremost clay minerals present in Nukhul Formation are montmorillonite and kaolinite. In Rudeis Formation, the main clay minerals is montmorillonite. Geochemically, the studied sections are characterized by higher percentage of SiO₂ and Fe₂O₃ in iron-rich sand. SiO₂, Fe₂O₃ and Al₂O₃ gathering to form the ferruginous and glauconitic sandstone. The high content of SiO₂, Na₂O, Cl, CaO and SO₃ as main elements of compound together and forming gypsum and evaporitic sandstone. On the other hand, the high content of CaO and MgO gathering to give limestone, dolomitic limestone and dolomite. So, through the light on the geochemical conditions the two different formations are deposited.

© 2019 Jordan Journal of Earth and Environmental Sciences. All rights reserved

Keywords: Mineralogy, Geochemical Studies, Early Miocene, Sinai and Egypt.

1. Introduction

The Miocene rocks in the Gulf of Suez areas have been studied by several authors (Said and El Heiny, 1967; El-Bakry et al., 2010; Hewaidy et al., 2012; Al-Husseiny, 2012; Abd El-Hafez et al., 2015). The Miocene sediments in the study areas are located between latitudes 29° 14' and 29° 18' N and longitudes 32° 55' and 33° 00' in Wadi Gharandal section. El Markha section is located between latitudes 29° 00' and 29° 03' N and longitudes 33° 10' and 33° 16' (Fig. 1).

The Miocene sediments developed on both rifts and in the central sub-basins display two markedly contrast sedimentary facies, a marginal and a deeper marine. The deeper marine facies is subdivided into two major groups namely Gharandal and Ras Malaab. On the other hand, the marginal (costal) marine facies is divided into four formations from base to top, namely Abu Gerfan, Gharamul, Gemsa and Sarbut El- Gamal respectively (El-Azabi, 1997). The Early Miocene is started with the deposition of algal limestone that changed later into fan-conglomeritic facies under the effect of the tectonic events (Abul-Nasr and Salma, 1999). The Nukhul Formation is Last Oligocene – Early Miocene age implying the Suez rift system started in the Oligocene. This study is based on the results of a biostratigraphic study of the Nukhul Formation at Wadi Babaa (Hewaidy et al., 2012). The Lower Miocene rocks can be classified into clastic (sandstones and argillaceous) and non-clastic (carbonate rocks with thin

evaporitic intercalations). The microscopic examination revealed different sandstone microfacies types such as: quartz arenite, calcareous quartz arenite, ferruginous quartz arenite, evaporitic quartz arenite, glauconitic quartz arenite and ferruginous evaporitic quartz arenite. The carbonate microfacies types in the studied formations include sandy micrite, biosparite, foraminiferal biomicroite, dolo-biomicroite, dolosparite, dolostone, pelsparite, oo-biosparite and evaporitic dolomicroite (Abd El-Hafez et al., 2015). The present work aims to shed more light at the lithostratigraphical, mineralogical and geochemical properties to evaluate the influence of geochemical conditions on the mineralogical composition.

2. Materials and Methods

To achieve this target, samples were collected to represent the different mineralogical and geochemical conditions. These samples were studied as follows:

2.1 X-ray diffraction (XRD)

Sixty-seven samples were selected and analyzed by XRD to identify the mineralogical composition. The analysis was carried out at the Egyptian Geological Survey and Mining Authority (central laboratories sector), using automated powder diffractometer system of Philips type Pan Alytica X-pert-pro with Ni-filter, Cu-radiation ($\lambda=1.542 \text{ \AA}$) at 40kV, 30mA and a normal scanning speed 0.02°/S. The reflection peaks between $2\theta = 2^\circ$ and 60° were obtained for the un-oriented analysis and between (2° - 35°) 2θ for the

* Corresponding author e-mail: el_hariri@yahoo.com

oriented analysis. The identification of the powder samples is determined by qualitative and semi-quantitative analysis. On the other hand, the clay size ($< 2\mu\text{m}$) fraction (eighteen samples) of clay minerals (three mounted slides for each sample) were prepared. The corresponding d-spacing and

relative intensities (I/I°) were obtained and compared with the standard data of the ICDD/2010 files by using APD program. The interpretation takes place by using APD and PDF programs which contain Powder Diffraction and PDF-2 Database Sets 1-45.

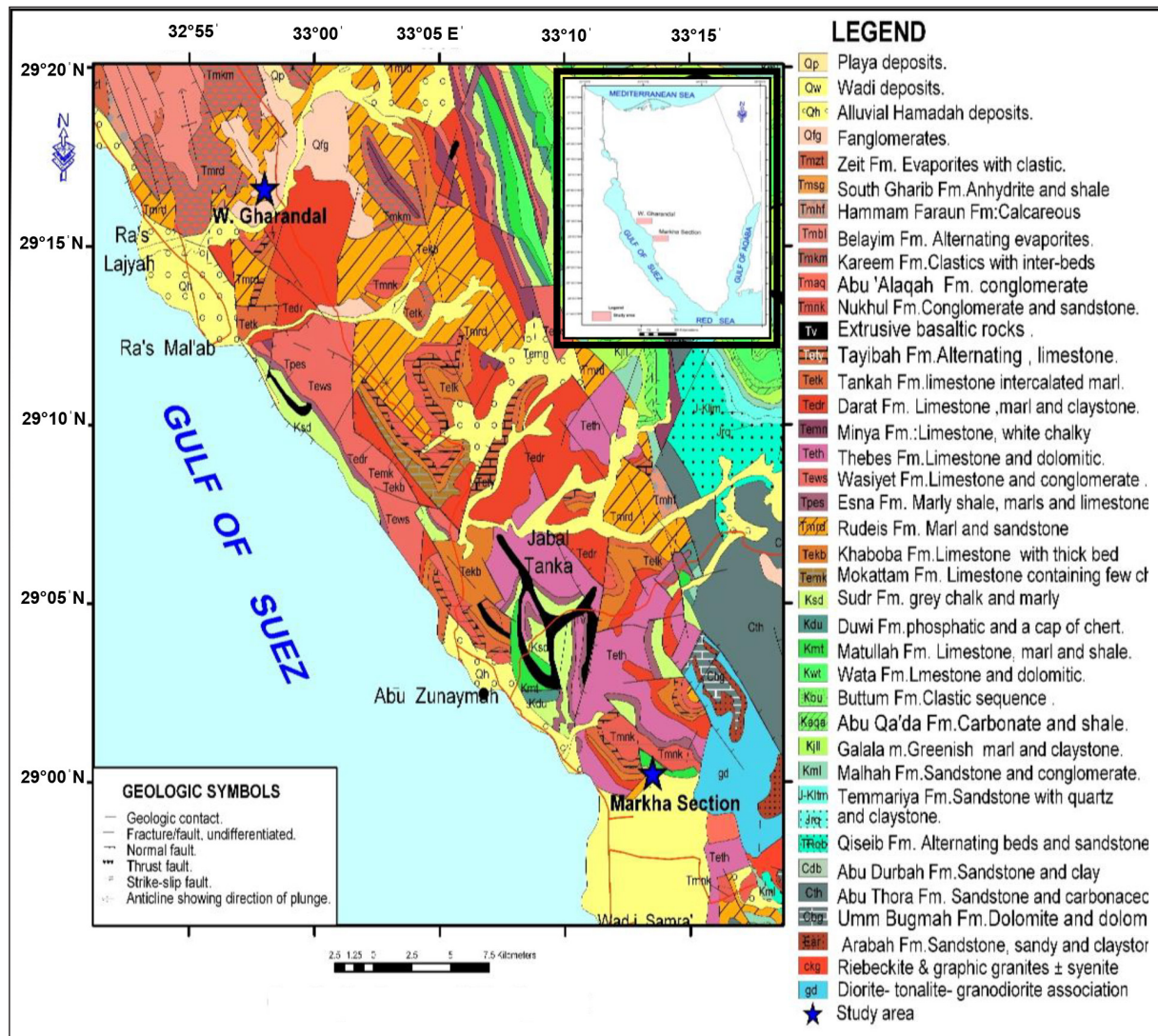


Figure 1. Location and geological map of the studied sections (After Conoco, 1986).

2.2 Scanning Electron Microscope (SEM)

Scanning electron microscopy (SEM) for four samples of different lithofacies was performed in order to understand the microstructure and diagenetic relationships among the pore spaces, main constituents and matrix of the studied sediments. Identification of the different minerals through SEM was facilitated by comparing their morphologic characteristics with those shown in the SEM petrology Atlas (Welton, 1984). SEM was carried out at the Egyptian Geological Survey and Mining Authority (central laboratory sector), using a SEM Model Philips XL30 attached with EDX units, with an accelerating voltage of 30 KV., magnification 10x up to 400,000x and resolution for W. (3.5nm). The samples were coated with gold.

2.3 X-Ray Fluorescence (XRF)

Forty-two samples representing clastic and non-clastic rock units were chemically analyzed after grinding at the Egyptian Geological Survey and Mining Authority (central

laboratory sector) using X-Ray fluorescence apparatus Technique. Philips X-Ray fluorescence equipment, model Philips PW/2404 and six analyzing crystals were used for determining major and trace elements. The maximum power of the equipment was 30 K.wt., Crystals (LIF-200), (LIF-220).

2.4 Statistical Analysis

The statistical studies were carried out using principally the SPSS (statistical Package for Social Science) program. The geochemical data were interpreted, and the factor analysis has been used by several investigators (Tamish, 1988) among other authors.

3. Lithostratigraphy

The lower Miocene in the Gulf of Suez and West Central Sinai is generally represented by two distinct facies, the marine facies and the non-marine or coastal facies. The variation of the environment is attributed to sea level changes that have

been overprinted twice by two major tectonic movements: the mid-Rudies and post-Kareem event (Abul-Nasr et al., 1999). The Nukhal Formation in the studied section is represented by limestone, sandstone and shales. Limestones are grayish white to yellow in color, massive, siliceous, hard, compact, dolomitic and fossiliferous lithofacies. Sandstones are yellow to reddish brown, compact, ferruginous, argillaceous with some salt intercalation. Shales are yellow brown to grayish in color, compact with veinlets of evaporities (Abd El-Hafez, 1986). The Rudeis Formation is formed of shale, sandstone and limestones. Shale are varicolored (greenish brown, grey, yellowish grey, yellowish brown and light grey) silty, semi-compact, ferruginous, calcareous, laminated high fossiliferous

lithofacies, (El-Bakry et al. 2010).

To achieve objectives of the present work, two early Miocene stratigraphic sections are represented; one in El-Markha and the second at Wadi Gharandal as follows:

3.1 El-Markha Section

The sedimentary succession of El-Markha section is represented by the Nukhul and Rudeis formations, which is about 170m thick together; Nukhul Formation is about 100m thick. It is unconformably capped by the Rudeis Formation which is 70m thick, and unconformably overlies Tayiba Formation of the Upper Oligocene. The Rudeis Formation is unconformably overlain by Kareem Formation of the Middle Miocene age (Fig. 2).

| Period | Epoch | Age | Rock units | | | | Thickness m. | Sample No. | Lithology | Description | | | |
|----------|-----------------|---------------|-------------|-------------|-------------|-------|--------------|------------|-----------|---|--|--|---|
| | | | Group | Formation | Member | | | | | | | | |
| | | | | | | | | | | | | | |
| Tertiary | Neogene | M. Miocene | Langhian | Ras Maalat | Kareem | Rhami | | | | Shale: Brown grey to brown compact, gypsum veinlets fissile, ferruginous and siliceous. | | | |
| | | | | | | | | | | | | | |
| | | Early Miocene | Burdigalian | Gharandal | Rudies | Mreir | Asl | | 24 | | Limestone: Yellowish white hard, compact, fossiliferous, evaporitic patch, brownish yellow sandstone in lower part. | | |
| | | | | | | | | | 11 | | 31-33 | | Shale: multi-colored (brown grey, brown, greenish grey), silty, semi compact, ferruginous, intercalation of yellow compacted limestone. |
| | | | | | | | | | 35 | | | | Sandstone: Yellowish to reddish brown, hard, compact, gypsiferous, evaporitic, intercalation of yellowish to brownish saltbed, brownish gray, silty, semi-compact and calcareous, ferruginous shale. |
| | Agaitantian | Nukhul | Gharandal | Mheiherratt | | | | 100 | | Limestone: Yellowish white, hard, compact, fossiliferous, reddish yellow ferruginous dolomite in the upper part. | | | |
| | | | | | | | | | | | | Sandstone: Yellowish to reddish brown, very dense, compact ferruginous rust-colored (bearing iron), argillaceous, intercalation of yellowish brown of salt bed. | |
| | Upper Oligocene | Chattian | Tayiba | Nukhul | Mheiherratt | | | | | | Limestone: Yellowish to white, massive, hard, compact fossiliferous, intercalation of reddish brown, to brownish yellow dolomite with brownish yellow, evaporitic sandstone with conglomerate bed at the base not exposure. | | |
| | | | | | | | | | | | | | |
| | | | | | | | | | | | | | |

Figure 2. Lithostratigraphic columnar section of Early Miocene sequence in El-Markha section, Southwest Sinai, Egypt.

3.2 Wadi Gharandal Section

In Wadi Gharandal section, the sedimentary units are about 325m thick. Nukhul Formation (ca. 90m thick) is unconformable and overlined by the Rudeis Formation (Mheiherratt Member) which is 235m thick and unconformable

overlying the Tanka Formation of Upper Eocene. Rudeis Formation is unconformably capped by the Kareem Formation which is related to the Middle Miocene age (Fig. 3). The studied areas can be subdivided into two formations from base to top as shown in Figure 3.

| Period | Epoch | Age | Rock units | | | Thickness m. | Sample No. | Lithology | Description | | | |
|----------|---------|---------------|-------------|-----------|-------------|--------------|------------|-----------|---|--|--|--|
| | | | Group | Formation | Member | | | | | | | |
| | | | | | | | | | | | | |
| Tertiary | Neogene | Early Miocene | Burdigalian | Gharandal | Ras Mha. | | | | Shale: varicolored (grey, brown and greenish yellow), silty, compact, some patches of gypsum & evaporates. | | | |
| | | | | | Kar. | | | | Limestone: grayish to yellowish, hard, massive, compact, with intercalation of evaporates mainly halite. | | | |
| | | | | | Mreir | | 31 m. | | Shale: multi-colored (yellowish brown, brownish to greenishgrey, light grey), with intercalation of evaporates mainly halite. | | | |
| | | | | | Asl | | 40 m. | 38-65 | Limestone: Yellowish white, hard, massive, fossiliferous, compact, with intercalation of evaporates mainly halite. Some of varicolored, yellowish brown, brownish to greenish grey, calcareous, semi-compact shale, with intercalated of brownish yellow, semi-friable sandstone | | | |
| | | | | | Mheiherratt | | 144 m. | 18-38 | Shale: varicolored (greenish brown, grey, yellowish grey, yellowish brown, light grey), hard, silty, semi-compact, cemented by calcareous clay, some evaporates, ferruginous, gypsum veinlets, intercalated with yellowish white, hard, compact, fossiliferous liestone. | | | |
| | | | | | Nukhul | | 90 m. | 1-17 | Sandstone: Brown yellow, fine to medium, semi-friable, ferruginous, calcareous, with brownish to grayish green, silty, semi-compacted shale in the upper part | | | |
| | | | | | | | | | Shale: Brownish to grayish, semi-compact, some brownish yellow, dense, ferruginous sandstone. Gypsum: yellowish white, coarsal crystalline, medium, compact trace of argillaceous with some intercalation of yellow compact limestone. | | | |
| | | | | | | | | | Conglomerate: brown to grey, hard, compact, underline by hard compact yellow limestone and brownish yellow to grey sandy shale bed. | | | |
| | | | | | | | | | | | | |
| | | | | | | | | | | | | |

Figure 3. Lithostratigraphic columnar section of Early Miocene sequence in Wadi Gharandal section, Southwest Sinai, Egypt.

4. Results and Discussion

4.1 Mineralogy

4.1.1 Mineralogical Composition of the Bulk Samples

Minerals identified from the bulk samples of the studied clastic sediments are illustrated in (Fig. 4). The obtained X-ray data were interpreted using American Society for Testing Materials (ASTM, 1960) data Cards together with data published by Brown (1961) and Deer et al., (1963). From this figure, it can be seen that quartz is the main mineral in the sandstone. Iron oxides mainly goethite and hematite represent the dominant mineral in the iron-rich sand and ferruginous

sandstone. Calcite is considered the main mineral in the calcareous sandstone, while montmorillonite and kaolinite were the main minerals in the argillaceous sandstone. The main constituting minerals in the evaporitic sandstone are represented by halite and gypsum. On the other hand, the non-clastic sediments represent calcite as a major mineral in carbonate (limestone) minerals, while dolomite is a secondary mineral in the dolomitic limestone and a major mineral in the dolomite samples (Fig. 4). Halite and gypsum are the major minerals in the evaporite minerals. Kaolinite, montmorillonite, quartz, iron oxides and some evaporite minerals are present as accessory minerals.

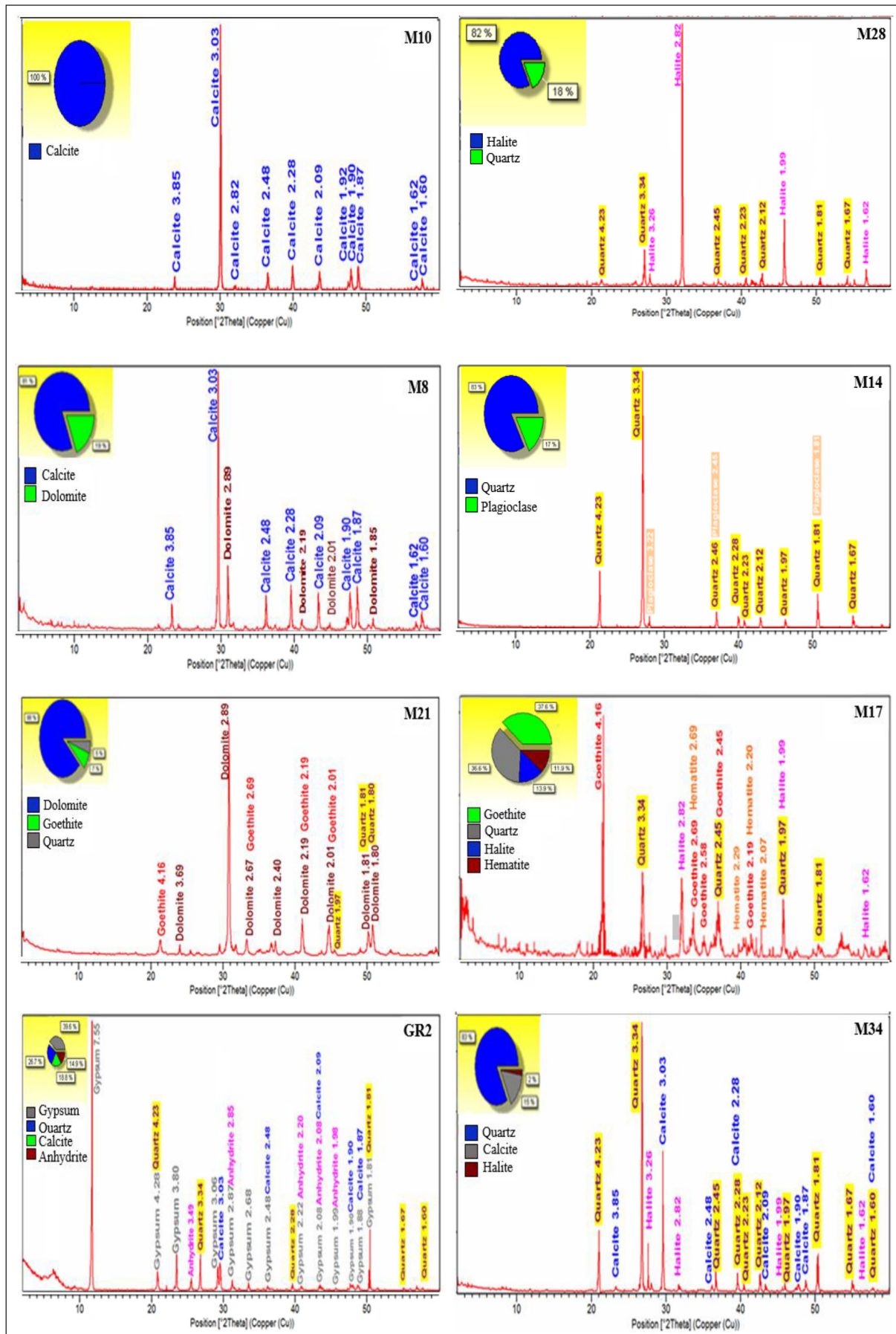


Figure 4. X-Ray Diffraction chart of the studied bulk samples of the studied sections.

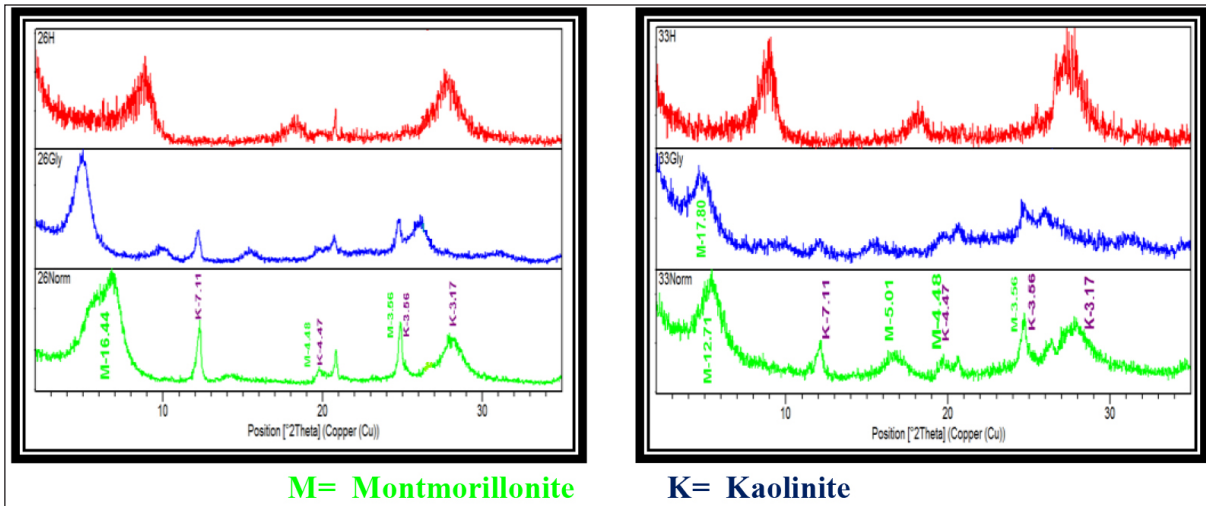


Figure 5. X-Ray Diffraction pattern of the studied clay rich samples in El-Markha section (Samples No. 26 and 33).

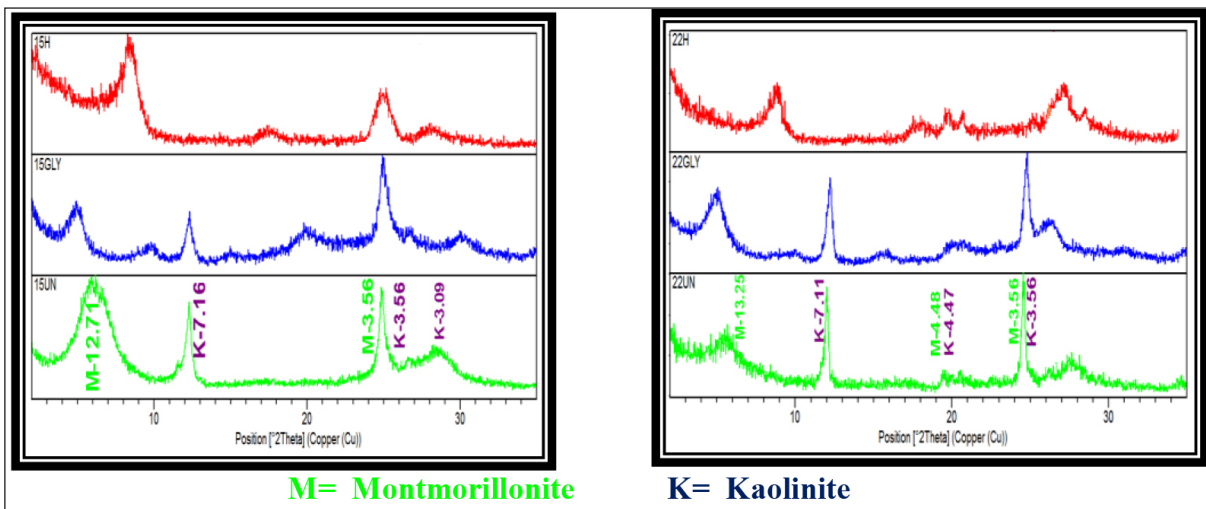


Figure 6. X-Ray Diffraction pattern of the studied clay rich samples in Wadi Gharandal section (Samples No. 15 and 22).

Montmorillonite is the most common mineral in shale of all rock units. Nukhul Formation samples contain montmorillonite about (52.63-72.03 %) with an average 60.91 %, while the samples of the Rudeis Formation are composed of (31.27-85.26 %) with an average 60.95 % of this mineral, (Figs. 5, 6, and 11).

Kaolinite is the most minor mineral in shale of all rock units excluding two samples (19 and 44) of the Rudeis Formation at Wadi Gharandal section where it is the main component. Nukhul Formation contains 27.97-47.37% with an average of 39.09% while Rudeis Formation contains of 14.74-68.73% kaolinite with an average of 39.05% (Figures 5, 6 and 10).

4.1.2 Semi-quantitative determination of clay minerals

The semi-quantitative analysis of the studied samples is shown in Tables (1 and 2) and Figures (7 and 8). This method is mentioned by Pierce and Siegel (1969) and Siegel et al., (1981) to detect the clay minerals by using the peak height of the strongest reflections of the individual clay minerals.

Table 1. Relative frequency distribution of the detected clay minerals (wt. %) in the studied samples (El-Markha section).

| Age | For. | Mem. | S.No | Montmorillonite | Kaolinite |
|---------------|--------|------|------|-----------------|-----------|
| Early Miocene | Rudeis | Asl | 33 | 85.71 | 14.29 |
| | | | 31 | 75.68 | 24.32 |
| | Hawara | | 26 | 82.76 | 17.24 |
| | | | 22 | 57.14 | 42.86 |

Table 2. Relative frequency distribution of the detected clay minerals (wt. %) in the studied samples (Wadi Gharandal section).

| Age | For. | Mem. | S.No. | Montmorillonite | Kaolinite |
|---------------|--------|--------|-------|-----------------|-----------|
| Early Miocene | Rudeis | Asl | 44 | 31.27 | 68.73 |
| | | | 38 | 85.26 | 14.74 |
| | | Hawara | 36 | 82.76 | 17.24 |
| | | | 32 | 76.1 | 23.9 |
| | | | 29 | 52.94 | 47.06 |
| | | | 22 | 60.53 | 39.47 |
| | | | 19 | 44.37 | 55.63 |
| | | | 18 | 54.4 | 45.6 |
| | Nukhul | 17 | 72.03 | 27.97 | |
| | | 16 | 70.92 | 29.08 | |
| | | 15 | 56.9 | 43.1 | |
| | | 10 | 57.98 | 42.02 | |
| | | 8 | 52.63 | 47.37 | |
| | | 6 | 55 | 45 | |

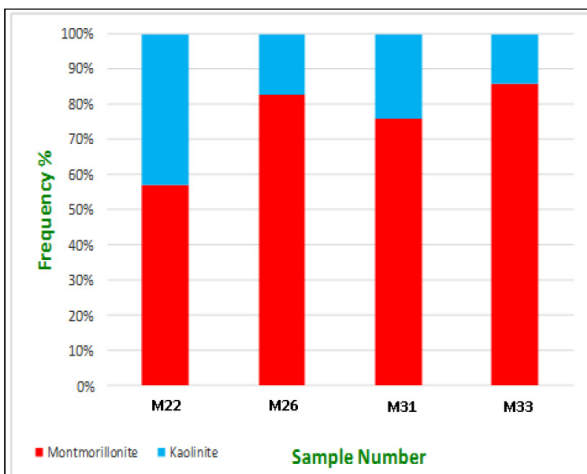


Figure 7. Frequency distribution of the detected clay minerals in the studied samples (El-Markha section).

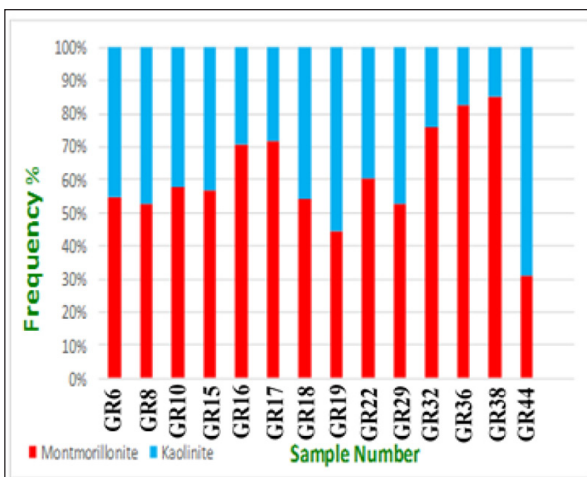


Figure 8. Frequency distribution of the detected clay minerals in the studied samples (Wadi Gharandal section).

4.1.3 Mineralogical Composition by Scanning Electron Microscopy

A petrographical study when combined with scanning electron microscope (SEM) investigations (Figs. 9, 10, 11, and 12) provides a good mean in identifying the mineralogical characteristics and the diagenetic process affecting the rock forming minerals. (El-Hariri, 2008 and Mousa et al., 2009).

The following SEM study is used to illustrate and identify the authigenic minerals, pore geometry and diagenetic events produced by different environments for examining sandstone, limestone, and clay minerals (Nukhul and Rudeis formations):

- 1- Dolomite crystal is shown in Figure 9, sample No. 4, Nukhul Formation at Markha section.
- 2- Kolinit is shown in Figure 10, sample No. 27, Rudeis Formation at Wadi Gharandal section.
- 3- Montmorillonite is shown in Figure 11, sample No. 27, Rudeis Formation at Wadi Gharandal section.
- 4- Iron oxides (Hematite and goethite in Figure 12, Sample No. 16, Nukhul Formation (El-Markha section).

5. Geochemical Composition

The main objective of the geochemical studies is to investigate the compositional variations of the studied samples and the vertical and lateral changes of the major and trace constituents and its mutual relationship. The following discussion is focused on the major and trace element response to the physicochemical conditions and deals with the abundance and distribution of these elements.

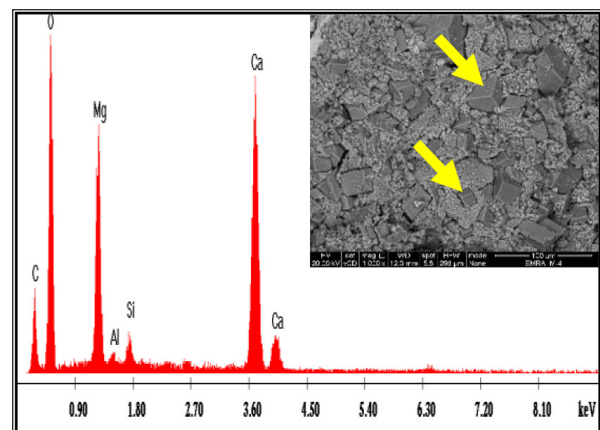


Figure 9. EDX and SEM photomicrograph showing dolomite crystals (arrows). Sample No. 4, Nukhul Formation (El-Markha section).

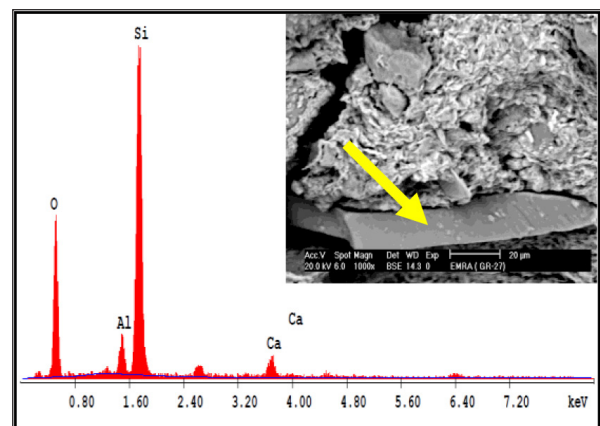


Figure 10. EDX and SEM photomicrograph showing kaolinite (arrow). Sample No. 27, Rudeis Formation (Wadi Gharandal section).

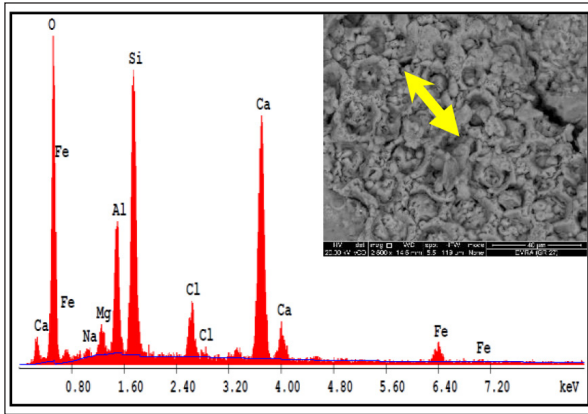


Figure 11. EDX and SEM photomicrograph showing montmorillonite mineral (arrow). Sample No. 27, Rudeis Formation (Wadi Gharandal section).

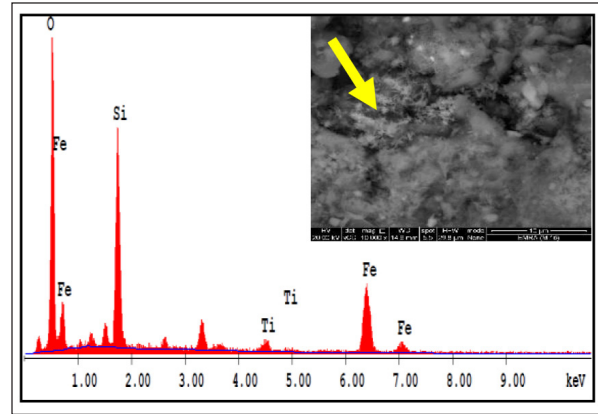


Figure 12. EDX and SEM photomicrograph showing iron oxides (goethite & hematite) (arrow). Sample No. 16, Nukhul Formation (El-Markha section).

Forty-two samples representing El-Markha and Wadi Gharandal sections were chemically analyzed for their major and trace elements.

The obtained data of both major and trace element constituents in the studied Early Miocene rocks with the average composition of each rock unit is given in Tables 3

and 4. The average composition of each studied rock unit is compared with those reported by other workers as shown in Table 5. The vertical distributions of the elements in the studied Lower Miocene successions are shown in Figures 13 and 14. The cluster analysis from the studied two sections are shown in Figure 15.

Table 3. Major oxides in wt. % and Trace elements in ppm of the Early Miocene rocks (El-Markha section).

| Age | Rock units | | S. No. | Major element oxides % | | | | | | | | | | | | | Ba | Sr | Cr |
|---------------|-------------|--------|--------|------------------------|------------------|--------------------------------|--------------------------------|-------|-------|-------|------------------|-------------------|-------------------------------|-----------------|-------|-------|-------|-------|-------|
| | Form. | Mem. | | SiO ₂ | TiO ₂ | Al ₂ O ₃ | Fe ₂ O ₃ | MnO | MgO | CaO | K ₂ O | Na ₂ O | P ₂ O ₅ | SO ₃ | Cl | L.O.I | | | |
| Early Miocene | Burdigalian | Rudeis | M38 | 17.02 | 0.18 | 2.79 | 1.64 | 0.02 | 5.22 | 32.8 | 0.23 | 3.01 | 0.13 | 0.4 | 2.12 | 34.16 | 430.9 | 257.9 | 64.8 |
| | | | M35 | 16.22 | 0.38 | 4.35 | 5.04 | 0.13 | 7.8 | 27.42 | 0.45 | 4.5 | 0.21 | 0.3 | 3.13 | 30.07 | 452.6 | 184.9 | 148.1 |
| | | | M34 | 55.01 | 0.65 | 2.9 | 2.26 | 0.06 | 1.47 | 17.41 | 0.78 | 2.81 | 0.15 | 0.4 | 1.9 | 14.03 | 464.3 | 270.1 | 66.6 |
| | | | M33 | 44.2 | 0.81 | 17.25 | 4.05 | 0.01 | 6.01 | 1.04 | 0.84 | 7.72 | 0.05 | 0.7 | 6.92 | 10.15 | 502.4 | 235.2 | 110.9 |
| | | | M32 | 2.49 | 0.04 | 0.26 | 1.27 | 0.12 | 0.69 | 53.2 | 0.02 | 0.32 | 0.14 | 0.2 | 0.08 | 4.09 | 348.3 | 152.5 | 28.5 |
| | | M31 | 47.32 | 0.89 | 18.65 | 2.93 | 0.01 | 2.66 | 1.26 | 0.41 | 9.15 | 0.09 | 0 | 8.21 | 8.07 | 530.4 | 209.5 | 117 | |
| | | M30 | 39.91 | 0.58 | 4.1 | 8.66 | 0.01 | 3.23 | 0.79 | 0.5 | 15.2 | 0.12 | 0.3 | 13.9 | 12.68 | 504.7 | 175.5 | 285 | |
| | | M29 | 34.84 | 0.15 | 2.63 | 8.13 | 0.34 | 3.14 | 2.4 | 0.4 | 10.52 | 0.24 | 0.3 | 12 | 24.55 | 372 | 118.8 | 11.2 | |
| | | M28 | 16.24 | 0.17 | 4.72 | 2.69 | 0.03 | 2.31 | 0.97 | 0.42 | 19.03 | 0.09 | 0.4 | 17.7 | 35.28 | 425.1 | 118.7 | 106.1 | |
| | | M26 | 45.75 | 0.86 | 16.2 | 3.67 | 0.01 | 5.65 | 0.32 | 0.54 | 5.57 | 0.05 | 0.3 | 7.04 | 13.98 | 558.3 | 132.9 | 108.7 | |
| | M24 | 22.46 | 0.36 | 7.48 | 2.65 | 0.02 | 0.81 | 0.22 | 0.25 | 18.33 | 0.05 | 1.2 | 17.5 | 28.54 | 444.4 | 106.6 | 77.1 | | |
| | M23 | 73.28 | 0.71 | 12.75 | 2.94 | 0.03 | 1.47 | 0.65 | 1.46 | 1.9 | 0.1 | 0.1 | 1.1 | 3.42 | 619.8 | 117.6 | 103.4 | | |
| | M22 | 49.85 | 1.18 | 19.35 | 3.99 | 0.01 | 4.15 | 3.85 | 0.83 | 1.48 | 0.01 | 0.1 | 2.33 | 12.8 | 583.9 | 277.1 | 116.9 | | |
| | A ver. | 35.74 | 0.535 | 8.73 | 3.84 | 0.062 | 3.435 | 10.95 | 0.548 | 7.656 | 0.11 | 0.3 | 7.21 | 20.66 | 479.8 | 181.3 | 103.4 | | |
| | Aquitanian | Nukhul | M21 | 4.7 | 0.04 | 0.42 | 7.12 | 0.37 | 22.15 | 23.8 | 0.07 | 0.4 | 0.07 | 0.5 | 0.8 | 39.3 | 317.9 | 113 | 57 |
| | | | M20 | 6.7 | 0.06 | 0.83 | 14.6 | 0.36 | 3.86 | 35.79 | 0.27 | 2.25 | 0.35 | 0.3 | 3.53 | 31.02 | 245.7 | 95.5 | 87.6 |
| | | | M19 | 42.7 | 0.31 | 6.32 | 8.64 | 0.09 | 2.46 | 1.07 | 0.39 | 11.1 | 0.14 | 0.8 | 10.2 | 15.49 | 376.7 | 105.3 | 74.2 |
| | | | M17 | 16.16 | 0.11 | 0.99 | 47.65 | 0.74 | 1.71 | 2.25 | 0.05 | 3.87 | 1.17 | 0.7 | 5.82 | 21.48 | 196.2 | 57 | 125.9 |
| | | | M16 | 48.83 | 0.69 | 0.46 | 10.39 | 0.3 | 1.59 | 0.82 | 0.68 | 11.41 | 0.07 | 0.1 | 12.9 | 11.5 | 432.9 | 96.2 | 103.6 |
| | | | M13 | 21.1 | 0.26 | 0.26 | 3.35 | 0.08 | 0.86 | 5.69 | 0.59 | 21.15 | 0.12 | 1.3 | 24 | 20.96 | 418.2 | 88.9 | 57.3 |
| M10 | | | 0.26 | 0.01 | 0.08 | 0.46 | 0.05 | 0.23 | 54.57 | 0.06 | 0.23 | 0.14 | 0.6 | 0.26 | 42.75 | 329.9 | 166.2 | 31.11 | |
| M8 | | | 0.54 | 0.01 | 0.04 | 1.33 | 0.05 | 3.85 | 52.4 | 0.01 | 0.02 | 0.12 | 0.8 | 0.01 | 40.54 | 337.6 | 175.2 | 32.1 | |
| M4 | | | 4.21 | 0.12 | 0.34 | 0.5 | 0.07 | 22.01 | 26.75 | 0.55 | 2.8 | 0.08 | 0.4 | 2.1 | 40.01 | 376.6 | 178.3 | 43.2 | |
| M3 | | | 44.43 | 0.71 | 4.13 | 2.46 | 0.02 | 1.86 | 2.7 | 1.38 | 12.8 | 0.21 | 1.7 | 15.1 | 12.23 | 547.8 | 439.7 | 71 | |
| M2 | 2.23 | 0.01 | 0.08 | 0.44 | 0.02 | 0.52 | 53.93 | 0.04 | 0.01 | 0.1 | 0.6 | 0.01 | 41.78 | 340.2 | 236.4 | 28.4 | | | |
| M1 | 12.4 | 0.05 | 1.2 | 3.01 | 0.12 | 4.27 | 39.2 | 0.01 | 2.03 | 0.34 | 0.5 | 2.4 | 34.3 | 330.8 | 152.9 | 39.1 | | | |
| A ver. | 17.022 | 0.198 | 1.26 | 8.33 | 0.19 | 5.44 | 24.9 | 0.34 | 5.67 | 0.24 | 0.69 | 6.43 | 29.3 | 354.21 | 158.7 | 62.54 | | | |

The mineralogical and chemical composition of clastic sedimentary rocks is controlled by various factors, including:

- (1) The composition of their source rocks.
- (2) Environmental parameters influencing the weathering of source rocks (e.g., atmospheric chemistry, temperature, rainfall and topography).

Table 4. Major oxides in wt. % and Trace elements in ppm of the Early Miocene rocks (Wadi Gharandal).

| Age | Rock units | | S. No. | Major element oxides % | | | | | | | | | | | | | Trace | | | | |
|---------------|-------------|--------|--------|------------------------|------------------|--------------------------------|--------------------------------|-------|------|------|------------------|-------------------|-------------------------------|-----------------|-------|-------|--------|--------|-------|-------|-------|
| | Form. | Mem. | | SiO ₂ | TiO ₂ | Al ₂ O ₃ | Fe ₂ O ₃ | MnO | MgO | CaO | K ₂ O | Na ₂ O | P ₂ O ₅ | SO ₃ | Cl | L.O.I | Ba | Sr | Cr | Pb | Rb |
| Early Miocene | Burdigalian | Rudeis | GR63 | 1.01 | 0.02 | 0.21 | 0.24 | 0.01 | 1.03 | 53.1 | 0.01 | 0.52 | 0.06 | 0.2 | 0.53 | 42.7 | 337.8 | 394.5 | 36.3 | 15.5 | 48.4 |
| | | | GR59 | 24.6 | 0.82 | 9.44 | 4.51 | 0.03 | 1.28 | 5.68 | 0.42 | 23.42 | 0.07 | 1.5 | 16 | 11.88 | 492.3 | 390.4 | 116.8 | 22.7 | 83.5 |
| | | | GR53 | 2.05 | 0.04 | 0.56 | 0.36 | 0.01 | 1.27 | 50.5 | 0.06 | 0.51 | 0.17 | 0.2 | 1.29 | 42.56 | 345.1 | 407.9 | 37.4 | 15.6 | 50.2 |
| | | | GR49 | 15.7 | 0.12 | 2.5 | 1.01 | 0.02 | 1.15 | 34.9 | 0.14 | 5.69 | 0.42 | 0.5 | 5.54 | 32.01 | 424.5 | 446 | 63.1 | 19 | 61.4 |
| | | | GR45 | 9.83 | 0.17 | 2.7 | 1.72 | 0.05 | 1.85 | 38.2 | 0.2 | 1.61 | 1.07 | 3 | 5.87 | 33.7 | 383.4 | 486 | 57.3 | 17.2 | 55.1 |
| | | GR38 | 43.9 | 0.79 | 14.31 | 6.69 | 0.02 | 3.25 | 5.7 | 0.51 | 4.59 | 0.09 | 0.2 | 6.1 | 13.52 | 424.5 | 371.2 | 63.1 | 19 | 61.4 | |
| | | GR34 | 13.1 | 0.13 | 3.54 | 5.7 | 0.23 | 2.51 | 34.8 | 0.1 | 2.15 | 0.61 | 0.5 | 5.15 | 31.04 | 367.3 | 1660 | 45.1 | 21.1 | 69.7 | |
| | | GR29 | 39.1 | 0.82 | 14.02 | 5.7 | 0.05 | 2.58 | 8.58 | 0.56 | 7.41 | 0.1 | 0.2 | 8.1 | 12.38 | 435.8 | 361.3 | 95 | 20.2 | 75.2 | |
| | | GR25 | 41.4 | 0.89 | 16.76 | 5.78 | 0.02 | 3.94 | 9.7 | 0.61 | 3.4 | 0.11 | 0.1 | 5.72 | 11.24 | 392.2 | 374.7 | 88.4 | 20.6 | 81.3 | |
| | | A ver. | 21.2 | 0.42 | 7.11 | 3.52 | 0.05 | 2.1 | 26.8 | 0.29 | 5.477 | 0.3 | 0.7 | 6.03 | 25.67 | 400.3 | 543.6 | 66.9 | 18.99 | 65.13 | |
| | Aquitanian | Nukhul | GR17 | 40.4 | 0.97 | 17.18 | 5.58 | 0.03 | 3.95 | 2.5 | 0.59 | 5.56 | 0.06 | 0.1 | 7.56 | 15.15 | 494.6 | 263.1 | 126.1 | 23.2 | 92.1 |
| | | | GR15 | 41.5 | 1.08 | 16.07 | 5.49 | 0.02 | 2.1 | 1.5 | 0.67 | 13.08 | 0.05 | 0.1 | 8.17 | 9.7 | 499.7 | 167.3 | 128.6 | 23.1 | 91.9 |
| | | | GR11 | 9.18 | 0.17 | 2.75 | 11.6 | 0.39 | 2.23 | 29.5 | 0.16 | 2.11 | 1.3 | 0.5 | 4.83 | 34.87 | 328 | 706.9 | 64.8 | 15.3 | 48.1 |
| | | | GR10 | 45.9 | 0.71 | 17.39 | 3.86 | 0.01 | 1.21 | 0.96 | 0.46 | 8.4 | 0.04 | 0 | 6.43 | 13.8 | 490.7 | 176.2 | 130 | 23.1 | 95.6 |
| | | | GR9 | 9.89 | 0.19 | 3.05 | 5.6 | 0.16 | 2.3 | 34.5 | 0.15 | 2.01 | 0.94 | 1 | 4.6 | 35.15 | 360.1 | 663.5 | 56.6 | 17.7 | 52.8 |
| | | | GR6 | 43 | 0.65 | 16.12 | 4.6 | 0.04 | 1.21 | 1.13 | 0.38 | 7.9 | 0.05 | 0 | 12.1 | 12.53 | 480.1 | 174.6 | 133.6 | 23.2 | 94.2 |
| | | | GR2 | 20 | 0.16 | 2.5 | 1.9 | 0.04 | 2.26 | 35.4 | 0.14 | 1.9 | 0.14 | 20 | 2.33 | 13.35 | 596 | 594.4 | 61.4 | 18.5 | 58.2 |
| | | | GR1 | 14.2 | 0.25 | 3.11 | 2.26 | 0.33 | 1.15 | 32.1 | 0.28 | 4.01 | 0.09 | 0.1 | 5.63 | 36.18 | 458.9 | 366.1 | 87.7 | 20.8 | 74.9 |
| | | | A ver. | 28 | 0.52 | 9.77 | 5.11 | 0.128 | 2.05 | 17.2 | 0.35 | 5.62 | 0.333 | 2.71 | 6.46 | 21.34 | 463.51 | 389.01 | 98.6 | 20.61 | 75.98 |

- (3) Duration of weathering.
- (4) Transportation mechanisms of clastic material from source region to depocentre.
- (5) Depositional environment (e.g., marine versus fresh water).
- (6) Post-depositional processes (e.g., diagenesis, metamorphism) Hayashi et al., (1997).

Table 5. Average major and trace element contents in the studied different rock types compared with other works.

| Rock type | Author | Major oxides (%) | | | | | | | | | | |
|-----------|------------------------------|------------------|------------------|--------------------------------|--------------------------------|-----|------|------|------------------|-------------------|-------------------------------|-----------------|
| | | SiO ₂ | TiO ₂ | Al ₂ O ₃ | Fe ₂ O ₃ | MnO | MgO | CaO | K ₂ O | Na ₂ O | P ₂ O ₅ | SO ₃ |
| Carbonate | Turekian and Wedepohl (1961) | 5.1 | 0.1 | 0.8 | 0.5 | 0.1 | 7.8 | 42.3 | 0.7 | 0.1 | 0.2 | ND |
| | Ronov and Migdisov (1971) | 6.1 | ND | 1.5 | 1.4 | ND | 6.3 | 43.2 | ND | 0.2 | ND | ND |
| | Wedepohl (1978) | 8.3 | ND | 1.7 | 1.3 | ND | 7.4 | 39.7 | ND | 0.3 | ND | ND |
| | Wedepohl (1978) | ND | 0.0 | 0.4 | 0.5 | 0.1 | <6.0 | 38.9 | 0.3 | 0.1 | 0.1 | ND |
| | Present work | ND | 0.0 | 0.4 | 0.5 | 0.1 | <6.0 | 35.6 | 0.3 | 0.1 | 0.1 | ND |
| Sandstone | Turekian and Wedepohl (1961) | 7.9 | 0.1 | 1.6 | 3.5 | 0.1 | 4.7 | 39.3 | 0.2 | 1.9 | 0.4 | 0.6 |
| | Turekian and Wedepohl (1961) | 78.8 | 0.3 | 4.8 | 1.3 | ND | 1.2 | 5.5 | 1.3 | 0.5 | 0.0 | ND |
| | Wedepohl (1978) | ND | 0.2 | 2.5 | 1.5 | 1.1 | ND | 3.4 | 1.5 | 1.2 | 0.7 | ND |
| Shale | Wedepohl (1978) | 44.4 | 0.5 | 4.9 | 10.8 | 0.2 | 2.1 | 3.5 | 0.1 | 8.7 | 0.3 | 0.5 |
| | Turekian and Wedepohl (1961) | 15.6 | 0.8 | 15.1 | 6.7 | 0.1 | 2.5 | 3.1 | 3.1 | 1.2 | 0.3 | ND |
| | Wedepohl (1978) | ND | 0.9 | 8.2 | 2.5 | 6.6 | ND | 4.8 | 2.5 | 0.6 | 0.2 | ND |
| Shale | Present work | 43.8 | 0.9 | 16.7 | 4.8 | 0.0 | 3.3 | 3.3 | 0.6 | 6.8 | 0.1 | 0.2 |

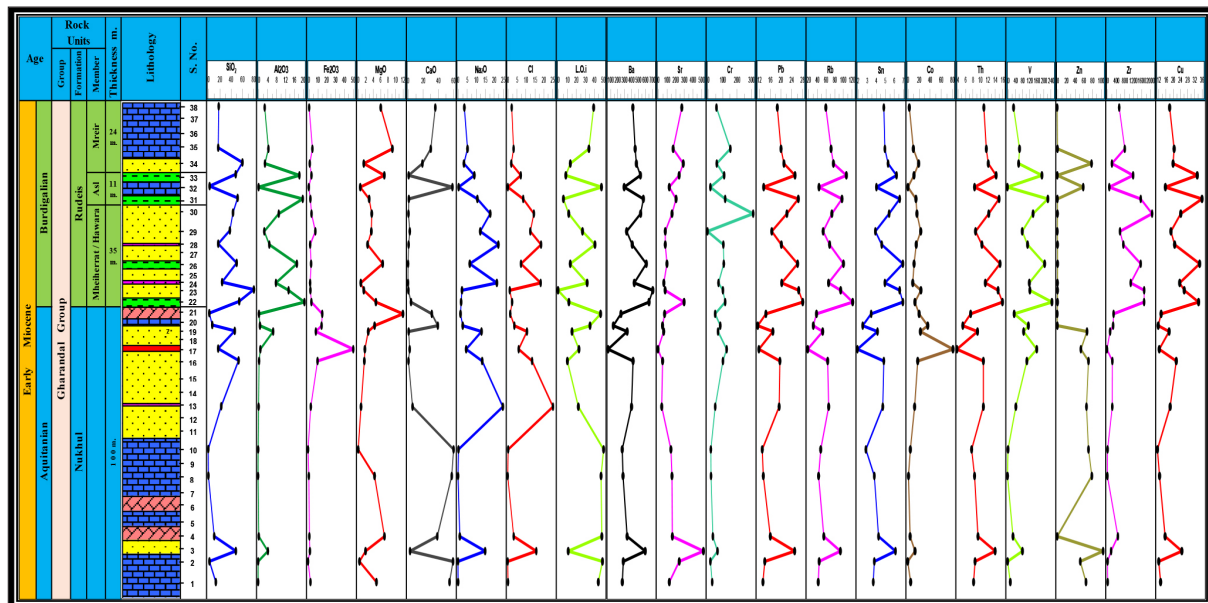


Figure 13. Chemo-stratigraphy of the different major and trace element constituents in Early Miocene rocks, El-Markha section.

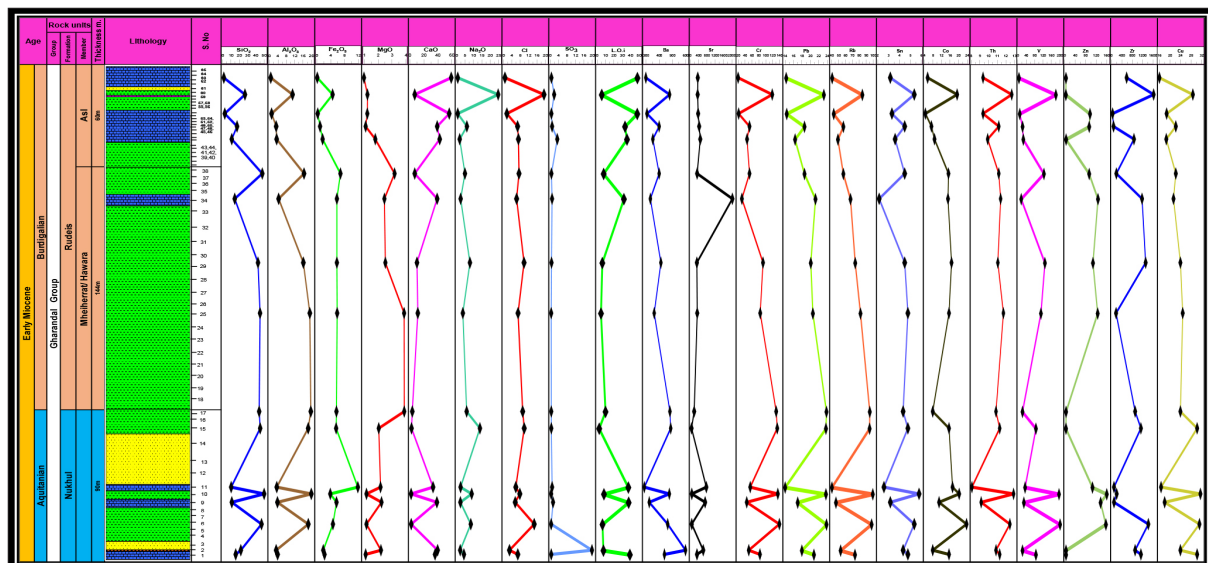


Figure 14. Chemo-stratigraphy of the different major and trace element constituents in Early Miocene rocks, Wadi Gharandal section.

6. Cluster Analysis

The cluster analysis of data obtained from X-ray fluorescence analysis is shown in Figure 15. These data represented the different various microfacies which indicate the presence of clastic sediments (Abd El-Hafez et al., 2015) such as quartz arenite, ferruginous quartz arenite, calcareous quartz arenite, iron-rich sand and shale and non-clastic rock units such as limestone, dolostone and gypsum. This type of analysis was performed by using cluster (SPSS) program.

Only two super-clusters, namely A and B were extracted representing all the different microfacies. The first super cluster (A) is Calcium oxides which are divided into two clusters (A₁ and A₂). The first one (A₁) consists of CaO, Zr, Sr and Br which are the main components of dolo-biomicroite, foraminiferal biomicroite, and biosparite microfacies (pure limestone). It is divided into four factors. The first factor includes CaO, MgO, Fe₂O₃, Zr, and Br which are all common components of (Dolostone) microfacies. The second factor consists of CaO, SO₃, S₁O₂, Ba, Sr and Zr which are all common components of the (Gypsum) factor. Factor number three include CaO and Fe₂O₃, Sr, Br and Zr which are the main components of Pelsparite and evaporitic dolomicroite microfacies (limestone). The last factor include CaO, SiO₂, Al₂O₃, Sr and Zr and Br which are all common components of Sandy micrite, foraminiferal biomicroite, and dolosparite microfacies (Sandy limestone).

The second super-cluster (B) is silicon dioxides which are divided into two clusters B₁ and B₂. The first cluster (B₁) is divided into two sub-clusters.

The first one (A₁) consists of CaO, Zr, Sr and Br which is the main components of dolo-biomicroite, foraminiferal biomicroite, and biosparite microfacies (pure limestone). The last one (A₁) is divided into four factors. The first factor involves CaO, MgO, Fe₂O₃, Zr and Br which are all common components of (Dolostone) microfacies. The second factor consists of CaO, SO₃, S₁O₂, Ba, Sr and Zr which are all common components of the (Gypsum) factor. Factor number three includes CaO and Fe₂O₃, Sr, Br and Zr which are the main components of Pelsparite and evaporitic dolomicroite microfacies (limestone). The last factor consists of CaO, SiO₂, Al₂O₃, Sr and Zr, and Br which are all common components of Sandy micrite, foraminiferal biomicroite, and dolosparite microfacies (Sandy limestone).

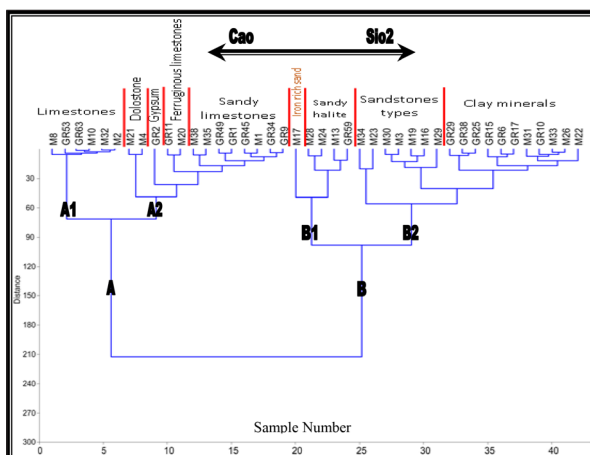


Figure 15. Cluster analysis of the Early Miocene rock units in studied areas, Southwest Sinai, Egypt.

The first one represented by SiO₂, Fe₂O₃, V, and Cr which include the main components of iron-rich sand. The second one includes SiO₂, Na₂O, Cl, Zr, Sr, and Ba which are the main common components of sandy halite bed. The second cluster (B₂) is divided into three factors. The first one includes the main components of calcareous quartz arenite and glauconitic quartz arenite such as SiO₂, Al₂O₃, CaO, Zr, and Br. The second factor is represented by SiO₂, Fe₂O₃, Na₂O, Cl, Zr, Br, Cr and, Sr of all common components of ferruginous evaporitic quartz arenite, Ferruginous quartz arenite and evaporitic quartz arenite microfacies. The last one is represented by SiO₂, Al₂O₃, Fe₂O₃, MgO, Zr, Br, Sr, V, Rb and Cr of all common components of clay minerals factors. The Montmorillonite is a main mineral while kaolinite is a minor mineral.

7. Conclusions

The present study is concerned primarily with exposed Early Miocene rocks in Southwestern Sinai along the Eastern side of the Gulf of Suez, at Wadi Gharandal and El-Markha sections. Both areas represented by the Nukhul and Rudeis formations. The Miocene succession variety in thickness ranges from 170 meters at El-Markha section to 325 meters at Wadi Gharandal section and is characterized by the presence of different rock types such as: sandstone, ferruginous sandstone, evaporitic sandstone, calcareous sandstone, iron-rich sand, evaporites, highly fossiliferous limestone, evaporitic limestone, dolostone, sandy limestone, dolomitic limestone and shale.

Mineralogically, the X-ray diffraction analysis of the Early Miocene sequence revealed the presence of calcite as the dominant minerals in the nonclastic rocks. Quartz was the dominant mineral in the clastic rocks, while goethite was the dominant mineral in the iron-rich sand, halite was the dominant mineral in the evaporite samples. Hematite, kaolinite, halite and gypsum are secondary minerals constituting the studied rock units with varying amounts.

The clay minerals in the studied samples of different formations were analyzed by the application of a semi-quantitative analysis which shows that the main clay minerals present in the Nukhul Formation are montmorillonite and kaolinite. In the Rudeis Formation, the main clay mineral is montmorillonite excluding two samples in which kaolinite is the main mineral.

From the data obtained by chemical analysis and the use of SPSS program it became clear that only two super-clusters namely (A and B) were extracted representing all the different microfacies. The first-super cluster (A) is Calcium oxides which are divided into two clusters (A₁ and A₂). The first one (A₁) consists of CaO, Zr, Sr, and Br which are the main components of dolo-biomicroite, foraminiferal biomicroite, and biosparite microfacies (pure limestone). The last one (A₁) is divided into four factors. The first factor involves CaO, MgO, Fe₂O₃, Zr, and Br which are all common components of (Dolostone) microfacies. The second factor consists of CaO, SO₃, S₁O₂, Ba, Sr and Zr which are all common components of the (Gypsum) factor. Factor number three includes CaO and Fe₂O₃, Sr, Br, and Zr which are the main components of Pelsparite and evaporitic dolomicroite microfacies (limestone).

The last factor includes CaO, SiO₂, Al₂O₃, Sr and Zr,

and Br which are all common components of Sandy micrite, foraminiferal biomicrite and dolosparite microfacies (Sandy limestone).

The second super cluster (B) is Silicon dioxides which are divided into two clusters (B₁ and B₂). The first cluster (B₁) divided into two sub-cluster. The first one which are represented by SiO₂, Fe₂O₃, V, and Cr which include the main components of (Iron-rich sand). The last one includes SiO₂, Na₂O, Cl, Zr, Sr, and Ba which are the main common components of (Sandy halite) bed. The second cluster (B₂) is divided into three factors. The first one includes the main components of (Calcareous quartz arenite and glauconitic quartz arenite) such as SiO₂, Al₂O₃, CaO, Zr and Br.

The second factor is represented by SiO₂, Fe₂O₃, Na₂O, Cl, Zr, Br, Cr, and Sr of all common components of (Ferruginous evaporitic quartz arenite, Ferruginous quartz arenite and evaporitic quartz arenite) microfacies.

The last one is represented by SiO₂, Al₂O₃, Fe₂O₃, MgO, Zr, Br, Sr, V, Rb and Cr of all common components of (Clay minerals) factors. Montmorillonite is a main mineral, while kaolinite is a minor mineral.

References

- Abd El-Hafez, N.A.M. (1986). Evaluation of petroleum prospect of some areas in the Gulf of Suez region. Ph. D., Al Azhar Univ. A. R. E., Cairo, p. 384.
- Abd El-Hafez, N.A.M., Abd El-Moghny, M.W., Ahmed Mousa, S.T., El-Hariri, Y. M., El-Din, H., Sharaka, K. (2015). Effect of diagenetic processes on storage capacity of Lower Miocene rocks at Southwestern Sinai, Egypt, *Intr. Jour. of Sci Eng. & App. Sci.*, 1(9): 2395-3470.
- Abul-Nasr, R.A., and Salama, G.R. (1999). Paleecology and depositional environments of the Miocene rocks in WESTERN Sinai, Egypt. M.E.R.C., Ain Shams Univ., Earth Sci. Ser., 13: 92-134.
- Al-Husseiny, M.I. (2012). Late Oligocene-Early Miocene Nukhul Sequence, Gulf of Suez and Red Sea. *Geo Arabia*, V. (17), pp. 17 - 44.
- American Society of Testing Material (1960). A.S.T.M., of X-Ray diffraction data, Amer. Soc. of Testing Materials, Phil., U.S.A., pp. 1119 - 1129.
- Brown, C. (1961). The X-Ray identification and crystal structure of clay minerals. A symposium, the Mineralogical Soc., London, p. 544.
- Conoco (1986). Geological map of Egypt, Scale 1:500.000, 6 Sheets, with cooperation of Egyptian General Petroleum Corporation, Klitzsch, E., List, F.K. and Pohlmann, G. (Editors), Berlin, Cairo, Egypt.
- Deer, W.A. Howie, R.A. Zssman, J. (1963). "Rock forming minerals". non-silicates, V. (5), p. 1788. John Willey and Sons, New York.
- El-Azabi, M.H. (1997). The Miocene marginal marine facies and their equivalent deeper marine sediments in the Gulf of Suez, Egypt: A revised stratigraphic setting. *Egypt. J. Geol.*, 41(2A): 273-308.
- El-Bakry, H.M., Zahra, H.A., Khater, T.M., Fawwaz, S.E., Almoazamy, A.A. (2010). Geology of West Central Sinai, Egypt. *Geol. Surv. (Unpublished)*. Report No. 53, p. 61.
- El-Hariri, T.Y. (2008). Depositional environment and petrophysical studies on subsurface Devonian sediment from Faghur-1 well at Northwestern Desert. *Jour. App. Sci. Res.*, 4 (1): 65-75.
- Garnder, J.V., Deab, W.E., Alonso, B. (1990). Inorganic of surface sedimentsof the Ebro shelf and slop northwestern Mediterranean. *Mar. Geol.*, Amsterdam, (95): 225-245.
- Hayashi, M., Komiya, T., Nakamura, Y., Maruyama, S. (1997). Archean regional metamorphism of the Isua supracrustal belt, Southern West Greenland: Implication for a driving force for Archean plate tectonics. *International Geology Review*, 42: 1055-1115.
- Hewaidy, A.A., Farouk, S., Ayyad, H.M. (2012). Nukhul Formation in Wadi Baba, Southwest Sinai Peninsula, Egypt. *Gulf Petro Link, Bahrain, Geo Arabia*, 17(1): 103-120.
- Mousa, A.S., El-Hariri, T.Y., El-Meligy, W.M. (2009). Assessing the Influence of diagenetic processes at El-Gedida Mines, El-Bahariya Oasis, Egypt, *Australian Journal of Basic and Applied Sciences*, 3(3): 1749-1762.
- Pierce, J.W., and Siegel, F.R. (1969). Quantification in clay mineral studies to sediments and sedimentary rocks. *J. Sed. Petrol. Tulsa.*, (39): 187-193.
- Said, R., and El Heiny, I. (1967). "Planktonic foraminifera from the Miocene rocks of the Gulf of Suez region, Egypt", Cushman contribution from the Cushman foundation. Part (I), V. (XVIII), pp. 14-26.
- Siegel, F. R., Pierce, J. W. and Kostick, D. S. (1981). Suspensates and bottom sediments in the Chilean Archipelago. *Modern Geology.*, (7): 217-299.
- Tamish, M., (1988). "Geomathematical and geochemical studies on Egyptian phosphorite deposits". *Berliner Geowiss. Abh. (A)*, Berliner, pp 98- 97.
- Welton, J.E. (1984). "SEM Petrology Atlas". A.A.P.G., Chevron oil field research company, U.S.A., Methods in exploration series no. (4), p. 237.